

Marquette University
e-Publications@Marquette

Biological Sciences Faculty Research and
Publications

Biological Sciences, Department of

3-15-2003

fc177, a Minor dec-1 Proprotein, Is Necessary to Prevent Ectopic Aggregation of the Endochorion During Eggshell Assembly in *Drosophila*

Debra Kay Mauzy-Melitz
Marquette University

Gail L. Waring
Marquette University, gail.waring@marquette.edu

Accepted version. *Developmental Biology*, Vol. 255, No. 2 (March 15, 2003): 193-205. DOI. © 2003 Elsevier Science (USA). Used with permission.

Marquette University

e-Publications@Marquette

Biological Sciences Faculty Research and Publications/College of Arts and Sciences

This paper is NOT THE PUBLISHED VERSION; but the author's final, peer-reviewed manuscript. The published version may be accessed by following the link in the citation below.

Developmental Biology, Vol. 255, No. 2 (March 15, 2003): 193-205. [DOI](#). This article is © Elsevier and permission has been granted for this version to appear in [e-Publications@Marquette](#). Elsevier does not grant permission for this article to be further copied/distributed or hosted elsewhere without the express permission from Elsevier.

fc177, a minor dec-1 proprotein, is necessary to prevent ectopic aggregation of the endochorion during eggshell assembly in *Drosophila*

Debra Mauzy-Melitz

Department of Biological Sciences, Marquette University, Milwaukee, WI

Gail L. Waring

Department of Biological Sciences, Marquette University, Milwaukee, WI

Abstract

The [Drosophila](#) eggshell is a highly specialized [extracellular matrix](#) that forms between the oocyte and the surrounding epithelial follicle cells during late [oogenesis](#). The *dec-1* gene, which is required for proper eggshell assembly, produces three proproteins that are cleaved within the vitelline membrane layer to multiple derivatives. The different spatial distributions of the cleaved derivatives suggest that they play distinct roles in

eggshell assembly. Using extant *dec-1* mutations in conjunction with genetically engineered *dec-1* [transgenes](#), we show that, although all three *dec-1* proproteins, fc106, fc125, and fc177, are required for female fertility, gross morphological abnormalities in the eggshell are observed only in the absence of fc177. The coalescence of the roof, pillar, and floor substructures of the tripartite endochorion suggested that quantitatively minor fc177 derivatives are necessary to prevent ectopic aggregation of endochorion proteins during the assembly process. Expression of a fc177 [cDNA](#) in *dec-1* null mutants was sufficient to restore spaces within the endochorion layer. Fc177 may function as a [scaffolding protein](#) akin to those utilized in viral [morphogenesis](#).

Keywords

Extracellular assembly, Endochorion morphogenesis, *Drosophila*, *dec-1*, Protein aggregation, Female sterile mutants

Introduction

Extracellular matrices are intricate, precisely organized molecular networks that provide cells with biological information as well as a mechanical scaffold ([Aumailley and Gayraud, 1998](#)). Although several of their structural components have been identified and domains that are used for protein–protein interactions have been mapped, little is known about how these matrices are assembled in vivo ([Henry and Campbell, 1998](#)).

The *Drosophila* eggshell is a specialized extracellular matrix that forms between the oocyte and overlaying somatic follicle cells over a 30-h time period during the latter stages of oogenesis. Largely proteinaceous, the eggshell is a highly organized multilayered structure featuring regional as well as radial complexity ([Margaritis, 1985](#)). The oocyte proximal vitelline membrane is assembled during stages 9 and 10. A crystalline inner chorionic layer (ICL), tripartite endochorion, and nonproteinaceous exochorion are formed during stages 11–14 ([Margaritis, 1986](#)). Specialized anterior structures that include the micropyle, operculum, and dorsal respiratory appendages are elaborated during stages 12–14. Like other extracellular matrices, the eggshell serves protective functions. It has also been suggested that the vitelline membrane layer acts as a storage site for spatial determinants that are utilized during early embryogenesis ([Savant-Bhonsale and Montell 1993](#), [St. Johnston and Nusslein-Volhard 1992](#)). The size of the *Drosophila* eggshell coupled with the temporal resolution provided by oogenesis affords an opportunity to study, in vivo, the assembly of a complex extracellular architecture in a system that is amenable to morphological, genetic, and molecular analyses.

As part of our long-term goal to understand the molecular mechanisms that underlie eggshell morphogenesis, we have been studying mutants defective in eggshell assembly. A large number of independent mutations have been linked to the *defective chorion-1* (*dec-1*) locus ([Bauer and Waring 1987](#), [Gans et al 1975](#), [Komitopoulou et al 1988](#)). The *dec-1* gene produces three alternatively spliced mRNAs that encode proproteins of 106, 125, and 177 kDa (fc106, fc125, and fc177, respectively, where fc denotes its follicle cell origin). The proproteins are secreted by the follicle cells and become localized in the vitelline membrane layer, where they are cleaved to at least five distinct protein products ([Noguerón and Waring, 1995](#)). Although generated in the vitelline membrane layer, *dec-1* derivatives relocate in a product-specific manner to different regions of the mature eggshell ([Nogueron et al., 2000](#)). The diverse spatial localizations of the derivatives suggest that *dec-1* is a multifunctional locus.

Dec-1 null mutants [*fs(1)410* and *fs(1) 384*] are female sterile and produce collapsed eggs ([Bauer and Waring 1987](#), [Komitopoulou et al 1988](#)). Ultrastructural analyses of *dec-1* mutant eggshells revealed an abnormal ICL ([Margaritis et al., 1991](#)), an aberrant endochorion ([Bauer and Waring 1987](#), [Komitopoulou et al 1988](#)), and aggregates of chorionic material in the underlying vitelline membrane ([Bauer and Waring, 1987](#)). The complexity of the eggshell phenotype, like the immunolocalization data, is consistent with a multifunctional locus. Genetic data indicate that more than one *dec-1* proprotein is required for female fertility. The deficiency

chromosome, *Df(1)ct^{Ab1}*, contains a breakpoint within the *dec-1* locus, but retains sufficient *dec-1* DNA to encode fc106 (Waring et al., 1990). Although fc106 and its derivatives are produced, *Df(1)ct^{Ab1}/fs(1)410* heterozygotes are sterile, suggesting that other *dec-1* proproteins are required for fertility. A *dec-1* splicing mutant, *fs(1)1501*, only produces the fc125 and fc177 proproteins. While the *Df(1)ct^{Ab1}* and *fs(1)1501* alleles complement each other in *trans*, *fs(1)1501* does not complement *dec-1* null mutant alleles (Hawley and Waring, 1988). This suggests that, although not sufficient, fc106 is required for female fertility and presumably the assembly of a functional eggshell.

In this paper, we have created *dec-1* transgenes in which either fc125- or fc177-specific sequences are selectively removed. By analyzing the effects of these mutations in different *dec-1* backgrounds, we show that, while both fc125- and fc177-specific sequences are required for female fertility, an organized tripartite endochorion failed to form only in the absence of fc177. Conversely, although sterile, *dec-1* null mutants carrying a fc177 cDNA transgene produced eggshells with near wild type morphology. Taken together, our data suggest that fc177 is required to create cavities and prevent abnormal protein aggregation within the endochorion layer.

Materials and methods

Drosophila strains

The Oregon R wild type stock and the *dec-1* mutant alleles, *fs(1)410* and *fs(1)384*, have been described previously (Bauer and Waring 1987, Komitopoulou et al 1988). The *Df(1)ct^{Ab1}* deficiency chromosome and fc177 cDNA transgene utilized in this study have also been previously described (Hawley and Waring 1988, Nogueron et al 2000). The fc125TAA and fc177TAAG transformant lines were created as described below.

Construction of *dec-1* mutant transgenes

Fc125TAA

A premature termination codon (TAAG) and an ectopic *Bam*HI restriction site were inserted into the *dec-1* gene near the beginning of the fc125-specific open reading frame at positions 5045 and 5051 (Waring et al., 1990), respectively, with mutagenic PCR primers. Using a 1.4-kb *Sst*I⁴⁵⁸⁷–*Sma*I fragment cloned into a pGem-4 vector (Promega, Madison, WI) as template, two overlapping PCR fragments containing the ectopic *Bam*HI site and the premature termination codon were generated. A 0.4-kb *Sst*I–*Bam*HI PCR fragment was generated by using a 25-nt forward primer equivalent to pGem-4 C²⁷⁵⁶ to A²⁷⁸⁰ and a 31-nt reverse primer complementary to *dec-1* C⁵⁰²⁵ to C⁵⁰⁵⁴. A “T” was inserted after C⁵⁰⁴⁴ to generate a premature TAAG termination codon, and an “A” was inserted after G⁵⁰⁵¹ to generate the ectopic *Bam*HI site. The PCR product was cut with *Sst*I and *Bam*HI and subcloned into a *Sst*I/*Bam*HI cut pGem-7Z vector. An overlapping mutagenic primer extending from C⁵⁰⁴² to T⁵⁰⁶⁵ that contained the nt insertions which were used to generate the ectopic termination codon, and the *Bam*HI site was used in conjunction with a T7 pGem-4 primer complementary to T⁹⁷ to A¹¹⁶ to generate a 1.0-kb PCR fragment. The 1.0-kb fragment was digested with *Sma*I and *Bam*HI and inserted into the pGem-7Z *Sst*I/*Bam*HI subclone that had been digested with *Bam*HI and *Sma*I. A mutagenized 1.4-kb *Sst*I/*Sma*I fragment was excised from the pGem-7Z vector and interchanged with its wild type counterpart in a 6.3-kb *Xho*I⁴⁴³/*Bgl*II *dec-1* genomic fragment that had been subcloned into a modified pGem-11Z vector (*Sst*I site removed). Making use of the unique *Xba*I³¹⁶⁰ site within the *dec-1* gene and an *Apa*I site in the polylinker region, a 3.6-kb *Xba*I/*Apa*I fragment was excised and subcloned into a pBluescript vector (Stratagene, La Jolla, CA). Using an appropriately placed *Kpn*I site within the polylinker region, a 3.6-kb *Xba*I/*Kpn*I fragment containing the premature termination codon was exchanged with its wild type counterpart in a pCaSpeR 4 P-element rescue vector that contained the *dec-1* gene along with 1.9 kb of 5' and 1.0 kb of 3' flanking DNA (Nogueron et al., 2000).

Fc177TAAG

A double-stranded oligonucleotide containing cohesive *Xba*I ends, three in frame TAAG termination codons and an *Eco*RI site (CTAGATAAGTATAAGTAGAATTCTAAGTAT/TATTCATATTCATCTTAAGATTCATAGATC) was inserted at the unique *Xba*I site in the open reading frame of the *dec-1* rescue vector described above. The orientation of the oligonucleotide insertion was verified by DNA sequencing. The introduction of termination codons at the *Xba*I site truncated the fc177-specific open reading frame at Arg¹⁰³⁰, 45 amino acids into the 604-amino-acid fc177-specific C terminus.

The fc125TAA and fc177TAAG constructs were purified by using a Qiagen Plasmid Midi Kit (Qiagen, Valencia, CA), and each was coinjected with the “wings clipped” helper plasmid, p π 25.7wc, into *yw* preblastoderm embryos as described by [Spradling and Rubin \(1982\)](#). Flies that emerged from the injected embryos were crossed with *yw* mates. Transformed flies carrying the transposons were recovered, and after chromosomal linkage of the transgenes was established, homozygous “transgene” stocks were created and maintained.

Western blot analysis

Ovaries were dissected from 2- to 6-day-old females, and egg chambers were separated, staged, and solubilized in SDS-containing buffers as previously described ([Noguerón and Waring, 1995](#)). Proteins were separated on SDS polyacrylamide gels and transferred to nitrocellulose or PVDF membranes using a Trans-Blot apparatus with plate electrodes (BioRad Laboratories, Hercules, CA). The five antisera utilized in this study, Nfc106, Ns80, Cfc106, Nfc177, and Cfc177 (see [Fig. 2](#)), have been described previously ([Nogueron et al., 2000](#)). Unless stated otherwise, the primary antisera were used at 1/1000 dilutions. Antigen–antibody complexes were visualized indirectly following the addition of either ¹²⁵I-Protein A or goat anti-rabbit secondary antibodies conjugated to horseradish peroxidase (Sigma-Aldrich). For ¹²⁵I detection, blots were processed and exposed to film as previously described ([Noguerón and Waring, 1995](#)). Enhanced chemiluminescence detection was used for the HRP-conjugated antibodies. Blots were blocked at room temperature for 1 h in 5% nonfat dry milk dissolved in Tris-buffered saline (TBS), pH 7.4, containing 0.2% Tween 20. The blocking solution was removed, and blots were incubated for 1 h at room temperature with antiserum diluted in blocking buffer. After successive washes in TBS containing, (1) 0.05% Tween 20, (2) 0.5% Triton X-100, and (3) 0.05% Tween 20, blots were incubated with the HRP-conjugated secondary antibodies (1/10,000 dilution in blocking buffer), washed as described above, incubated for 1 min with standard ECL reagents, and exposed to film. For reprobing with different antibodies, the nitrocellulose membranes were placed in TBS containing 0.7% β -mercaptoethanol and 2% SDS for 30 min at room temperature. Following a 30-minute wash in TBS, the membranes were blocked and processed as described above.

Morphological analyses

Ovarian tissue was fixed overnight at 4°C in 2% glutaraldehyde in 0.1 M sodium cacodylate, pH 7.4, rinsed, postfixed in 1% osmium tetroxide for 2 h, dehydrated, and infiltrated with Spurr resin, unless indicated otherwise. Thin sections were cut with glass knives and a Sorvall Porter-Blum MT-2B ultramicrotome, collected on copper grids, stained with lead citrate and uranyl acetate, and viewed with a Hitachi H600 transmission electron microscope housed in the Imaging facility at the University of Wisconsin, Milwaukee. Scanned TEM were manipulated with Adobe PhotoShop software.

For light microscopy, semithin sections (150–250 nm) were transferred to glass slides and stained with 1% Toluidine O in 1% sodium borate.

Results

The *fc106 dec-1* proprotein and its derivatives are not sufficient to organize a tripartite endochorion

Dec-1 products are necessary to form an organized and stable eggshell. During early stage 14, the vitelline membrane, inner chorionic layer (ICL), and tripartite endochorion layers, characteristic of the mature eggshell, are readily apparent in wild type egg chambers (Fig. 1A, A). In early stage 14 egg chambers from *dec-1* null mutants [e.g., *fs(1)410*] electron dense aggregates, reminiscent of endochorion pillars, accumulate between the follicle cells and the inner chorionic and vitelline membrane layers (Fig. 1A, B). As egg chamber development progresses, the electron dense aggregates coalesce into a continuous layer (Fig. 1A, C). Eventually, small aggregates of electron dense endochorionic material become dispersed throughout the vitelline membrane layer (Fig. 1A, D and E). As previously reported for *fs(1)384* (Komitopoulou et al., 1988), clumped endochorionic material was also observed in the interior of the dorsal respiratory appendages of the *fs(1)410* mutant (Fig. 1B, B). Defects in the crystalline substructure of the ICL in *fs(1)384 dec-1* null mutants have been reported (Margaritis et al., 1991). In agreement with abnormal morphogenesis of this layer, we consistently observed an abnormal association of the ICL with the vitelline membrane in the *dec-1* protein null mutants (Fig. 1A, B–E).

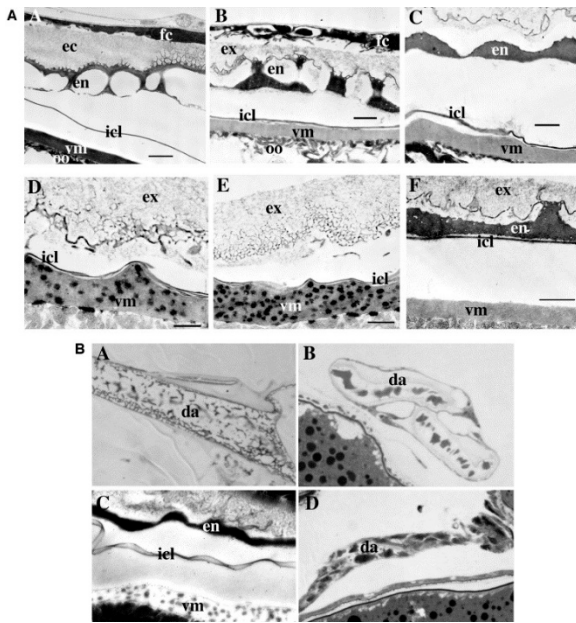


Fig. 1. (A) Transmission electron micrographs of the eggshell in the main body region of wild type and *dec-1*-deficient egg chambers. (A) Early wild-type stage 14 egg chamber. (B–D) Progressive collapse of endochorion in early, mid, and late stage 14 egg chambers, respectively, from *fs(1)410 dec-1* null females; (E) late stage 14 egg chamber from *fs(1)384 dec-1* null mutant; (F) late stage 14 egg chamber from a *Df(1)ct^{4b1}/fs(1)410* heterozygote which produces only *fc106* and its derivatives. *fc*, follicle cells; *ex*, nonproteinaceous exochorion layer; *en*, endochorion; *icl*, inner chorionic layer; *vm*, vitelline membrane; *oo*, oocyte. The bar represents one micron. (B) Dorsal appendage morphology in wild type and *dec-1*-deficient egg chambers. Light micrographs showing longitudinal sections through the dorsal appendage of (A) wild type, (B) *fs(1)410 dec-1* null, and (D) *Df(1)ct^{4b1}/fs(1)410* stage 14 egg chambers. (C) Transmission electron micrograph of the anterior region near the base of a dorsal appendage from a *Df(1)ct^{4b1}/fs(1)410* stage 14 egg chamber embedded in Lowicryl resin. *da*, dorsal appendage; *en*, endochorion; *icl*, inner chorionic layer; *vm*, vitelline membrane.

The *dec-1* gene produces three proproteins, fc106, fc125, and fc177 (Fig. 2 and Table 1), in varying amounts. In wild type egg chambers, the fc106 proprotein is approximately 10 times more abundant than either fc125 or fc177. In the mature egg chamber, the N-terminal fc106 derivative, s25, is localized in all three eggshell layers (endochorion, vitelline membrane, and ICL), while the C-terminal derivative, s60, is found in the vitelline membrane and endochorion layers. Because of their relative abundance and widespread distribution, the fc106 derivatives might be expected to play a major role in assembling an organized, tripartite endochorion, we examined *Df(1)ct^{Ab1}/fs(1)410* mutant egg chambers. The *Df(1)ct^{Ab1}* chromosome contains a breakpoint within the *dec-1* locus at position 3109 (Fig. 2), which leads to the production of a single truncated mRNA. Since the breakpoint lies 3' of the fc106 termination codon, fc106 and its derivatives are still produced (Waring et al., 1990; and Table 1). In most of the *Df(1)ct^{Ab1}/fs(1)410* stage 14 egg chambers examined, the endochorion appeared as a continuous, electron dense layer in close association with the ICL (Fig. 1A, F). Although a defined floor, pillar, and roof structure failed to form in the main body, unlike *dec-1* null mutants, electron dense aggregates were not observed in the underlying vitelline membrane. However, aggregates within the vitelline membrane were observed in sections near the base of the dorsal appendages (Fig. 1B, C). Such aggregates were not observed in stage 14 egg chambers from wild type or any of the other mutant females utilized in this study. Like the *dec-1* null mutants, electron dense accumulations were also apparent in the interior of the dorsal appendages (Fig. 1B, D). The partial morphological rescue of the *dec-1* null eggshell phenotype observed in *Df(1)ct^{Ab1}/fs(1)410* egg chambers indicates that fc106 products, while not sufficient to prevent the abnormal aggregation of endochorionic material between the follicle cells and ICL, are sufficient to prevent its collapse into the underlying vitelline membrane in the main body and prevent the abnormal association of the ICL with the vitelline membrane (Fig. 1A, F). Fc106 derivatives may provide a direct and critical role in endochorion stabilization, and/or the absence of endochorion aggregates in the vitelline membrane may be related to the more normal morphogenesis of the intervening ICL layer. The N-terminal derivative, s25, is the only *dec-1* derivative that localizes within the ICL (Nogueron et al., 2000). The more typical association of the ICL with the endochorion layer upon the introduction of fc106 derivatives is consistent with this localization data.

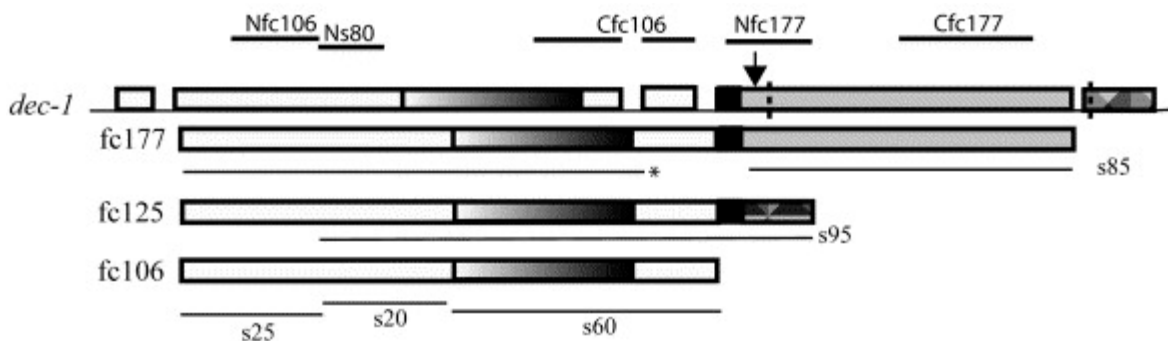


Fig. 2. The *dec-1* gene, its proproteins and cleaved derivatives. *dec-1* open reading frames are denoted by the rectangles; the 5' and 3' untranslated regions as well as introns are indicated by the lines. The open reading frames that comprise each of the three *dec-1* proproteins, fc177, fc125, and fc106, are shown below. The open rectangles indicate sequences that are common in all three proproteins. The shaded rectangle within this region indicates a glutamine, methionine-rich repeating motif described previously (Waring et al., 1990). The black box indicates sequences shared by fc125 and fc177; the gray rectangle shows fc177-specific sequences, while the patterned rectangle indicates fc125-specific sequences. The lines below the proproteins indicate the approximate regions that correspond to the cleaved derivatives s85, s95, s25, s20, and s60. The starred derivative represents the putative N-terminal derivative of fc177 (see text). The downward arrow indicates the position of the breakpoint that falls within the *dec-1* locus in the *Df(1)ct^{Ab1}* chromosome. The dashed vertical lines indicate the positions of the premature termination codons that were introduced into the fc177-specific

and fc125- specific open reading frames in the fc177TAAG and fc125TAA [transgenes](#), respectively. The lines above the *dec-1* gene show the regions that were used to generate the various [antisera](#) (Nfc106, Ns80; Cfc106, Nfc177, and Cfc177) used in this study.

Table 1. Dec-1 proprotein production

Allele or transgene	fc106	fc125	fc177
wild type	+	+	+
<i>fs(1)410;fs(1)384</i>	-	-	-
<i>Df(1)cf^{Ab1}</i>	+	-	-
<i>fs(1)1501</i>	-	+	+
Fc125TAA	+	-	+
Fc177TAAG	+	+	-
Fc177cDNA	-	-	+

Note. Listed are the *dec-1* mutant alleles and [transgenes](#) used or referred to in this study.

Eggshells with wild-type morphology are assembled in the absence of fc125-specific sequences

Ultrastructural analysis of *Df(1)ct^{Ab1}/fs(1)410* egg chambers confirmed that fc125- and/or fc177-specific sequences are required for proper eggshell morphology as well as female fertility. To separate the roles of these minor dec-1 proproteins in eggshell assembly, we selectively removed fc125-specific sequences. A premature termination codon was engineered into a *dec-1* transgene near the beginning of the fc125-specific open reading frame ([Fig. 2](#)). Normal versions of the fc106 and fc177 proproteins and their derivatives, and truncated versions of fc125 and its C-terminal derivative, s95, were expected from the engineered transgene ([Table 1](#)). The Cfc106 antiserum ([Fig. 3A](#)) was used to detect the C-terminal derivatives of fc106 (s80 and s60) and fc125 (s95), while the Cfc177 antiserum ([Fig. 3A](#)) was used to detect s85, the C-terminal derivative of fc177. A blot of staged egg chamber proteins from wild type and *dec-1* null females [*fs(1)410*] carrying two copies of the fc125TAA transgene was incubated with the Cfc106 antiserum ([Fig. 3B](#)). The profiles of the stage 10 egg chambers showed that, as expected, the null mutants with the fc125TAA transgene produced and processed fc106 in a wild type manner (lanes 3 vs 4, [Table 1](#)). In wild type stage 12 egg chambers, s95, s80, and small amounts of s60 accumulated (lane 5). Although the intensity of the s80 and s60 signals were comparable with wild type (lane 2 vs lane 5), s95 was not detected in mutant stage 12 egg chambers. An ectopic band in the expected molecular weight range of the truncated product (82 kDa) was not evident; however, a band in this size range could easily have been masked by the s80 signal. Processing of s80 to s60 is evident in both mutant (lane 1) and wild type (lane 6) stage 14 egg chambers. To test for fc177 production, the blot was stripped and reincubated with the Cfc177 serum. As shown in [Fig. 3C](#), s85 accumulation was similar in the wild type (lanes 5 and 6) and mutant (lanes 2 and 1) egg chambers. Taken together, these data indicate that fc125-specific sequences were not expressed by the fc125TAA transgene and that the absence of these sequences did not appear to affect accumulation or processing of the fc106 and fc177 proproteins.

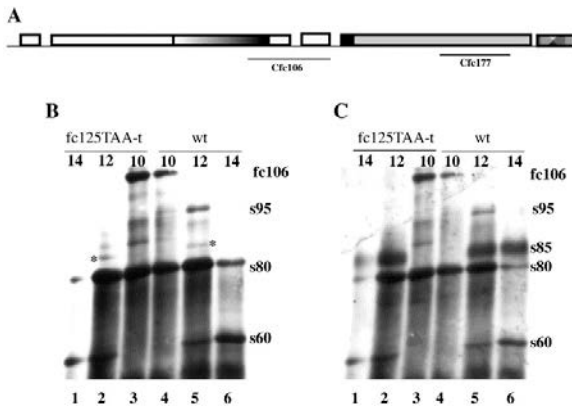


Fig. 3. [Western blot analysis](#) of *dec-1* null mutant egg chambers carrying two copies of the fc125TAA [transgene](#). (A) Diagram of the *dec-1* gene and the regions to which the [antisera](#) were directed. (B and C) SDS soluble egg chamber proteins from wild-type (wt) or *fs(1)410 dec-1* null females carrying two copies of the fc125TAA transgene (fc125TAA-t). The egg chamber stage is indicated at the top of each lane. (B) [Nitrocellulose](#) blot of egg chamber proteins recognized with the Cfc106 antiserum (1:5000 dilution) using ECL detection. (C) Blot shown in (B) stripped and reprobed with the Cfc177 antiserum. Although incomplete, the differences in exposure times (20 s in B vs 10 min in C) indicates that the stripping was efficient. The major, well-characterized *dec-1* proteins and derivatives are indicated to the right. The asterisk denotes a band whose migration is consistent with a [N-terminal](#) derivative of fc177 (see later discussion).

Ultrastructural analysis of late stage 14 egg chambers from *fs(1)410;fc125TAA* females displayed normal eggshell morphology ([Fig. 4](#)). The endochorion was organized into a classic tripartite structure, and the underlying vitelline membrane appeared as a homogenous layer ([Fig. 4A](#)) lacking the electron dense accumulations characteristic of *dec-1* null egg chambers. The ICL was associated with the endochorion rather than the vitelline membrane ([Fig. 4A](#)), and the reticular-like interior of the dorsal appendages ([Fig. 4B](#)) was similar to wild type ([Fig. 4C](#)). Although the morphology of the eggshell was similar to wild type, a functional eggshell was not assembled in the absence of the fc125-specific sequences. The fc125TAA transgene from two independent lines was not able to rescue the *dec-1* female sterile mutant phenotype. Furthermore, unlike wild type, eggs from *fs(1)410* and *fs(1)410;fc125TAA* females ruptured when dechorionated manually or when subjected to the weight of a coverslip, both hallmarks of structurally compromised, fragile eggshells. Perhaps the sterility associated with *fs(1)410;fc125TAA* females is a consequence of the inability of their fragile eggshells to withstand the physical pressures associated with ovulation and passage of the egg down the oviduct.



Fig. 4. Wild type eggshell morphology in *dec-1* null mutants carrying the fc125TAA [transgene](#). Transmission electron micrographs from the main body of the eggshell of a late stage 14 egg chamber (A) and the interior of a dorsal appendage at stage 14 (B) from *fs(1)410* females carrying two copies of the fc125TAA transgene. The interior of a dorsal appendage from wild-type stage 14 egg chambers is shown in (C). The bar indicates one micron. da, dorsal appendage; other abbreviations as in the legend to Fig. 1.

Fc177 is required for organization of a tripartite endochorion

Ultrastructural analyses of the *Df(1)ct^{Ab1}/fs(1)410* and *fs(1)410;fc125TAA* egg chambers showed that (1) the fc106 proprotein was not sufficient, and (2) the fc125 proprotein was not required, to form a tripartite endochorion. These data suggest that the minor fc177 proprotein plays a major role in endochorion

morphogenesis. Fc177 is synthesized during stages 11–12 and is processed in stages 12 and 13 to a fc177-specific C-terminal derivative, s85 (Noguerón and Waring, 1995). As s85 is generated, it becomes rapidly localized to the endochorionic cavities (Nogueron et al., 2000). The unique localization of s85 within the endochorionic cavities is compatible with a major role in endochorion formation. To investigate the significance of fc177-specific sequences, in-frame termination codons were inserted at the *Xba*I site between S¹⁰²⁹ and R¹⁰³⁰, yielding a fc177TAAG transgene with a putative translation product that included only 45 of the 604 fc177-specific amino acids (see Fig. 2). The Western blot shown in Fig. 5B confirms that the premature termination codons are utilized efficiently when the fc177TAAG transgene is introduced into *dec-1* null mutants. Unlike wild type (lanes 3 and 4), immunoreactive products were not detected in *fs(1)410 dec-1* null mutants containing the fc177TAAG transgene when appropriately staged egg chambers (lanes 1 and 2) were incubated with the Cfc177 antiserum (Fig. 5A). Immunoreactive products were also not detected with the Nfc177 serum (Fig. 5A), a serum that recognizes s85 in wild type egg chambers (data not shown). The results with both antisera are consistent with truncation of the fc177 specific C terminus.

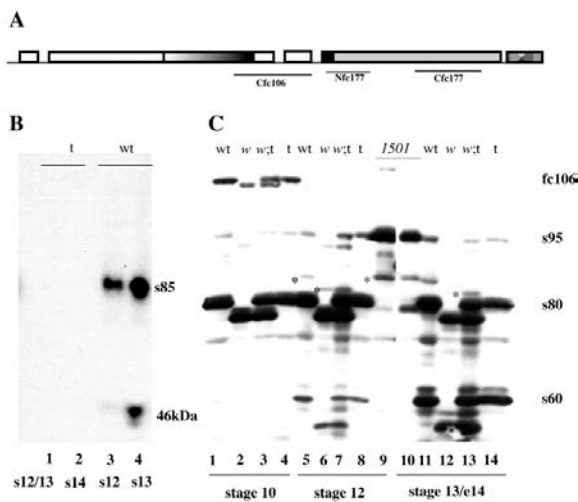


Fig. 5. [Western blot analysis](#) of *dec-1* null females carrying two copies of the fc177TAAG [transgene](#). (A) Diagram of the *dec-1* gene showing regions to which the [antisera](#) were directed. (B and C) SDS soluble egg chamber proteins from different [genotypes](#) at the stages of [oogenesis](#) indicated below each lane were separated on a 7.5% [polyacrylamide](#) gel. After transferring to [nitrocellulose](#), the blots were incubated with either the Cfc177 (B) or the Cfc106 (C) antiserum. (B) (70 egg chambers/lane): lanes 1 and 2, two copies of the fc177TAAG transgene from the 3.2.1 transformant line in *fs(1)384 dec-1* null mutant females (*t*); lanes 3 and 4, Oregon R, P2 strain wild type [flies](#) (*wt*). s85 and a 46-kDa fc177 C-terminal derivative were detected with ¹²⁵I-Protein A. (C) *wt* (lanes 1, 5, and 11) and *t* as in (B) (lanes 4, 8, and 14); lanes 2, 6, and 12—flies with a [white X chromosome](#) that produces electrophoretic variants of *dec-1* proteins (*w*); lanes 3, 7, and 13, *w* females carrying two copies of the fc177 TAAG transgene (*w;t*); lanes 9 and 10, *fs(1) 1501 dec-1* mutant flies (*1501*). In (C), reactive bands were detected by using ECL. The positions of the standard forms of fc106, s95, s80, and s60 are indicated to the right in (C). The bands with asterisks denote standard and variant forms of the putative fc177 [N-terminal](#) derivative (e.g., lanes 5, 6, 9, and 13).

To facilitate the analysis of the production of fc106, fc125, and more N-terminal fc177 derivative(s) by the fc177TAAG transgene, we made use of *dec-1* electrophoretic variants. The positions of the standard forms of fc106, s95, and s80 are shown in lanes 1 and 5 of Fig. 5C; s60 is shown in lane 11. Variant forms of these proteins are produced by the *dec-1* allele associated with the *white* (*w*) X chromosome used in our transformation experiments (lanes 2, 6, and 12). The concomitant increases in the mobilities of all four of these *dec-1* proteins in *w/w* females suggest a size polymorphism that arises from a small deletion in the *dec-1* gene in a region that

is common to all four proteins (e.g., s60 region). Stage 10 egg chambers from *w/w* females carrying two copies of the *fc177TAAG* transgene displayed both the standard and variant forms of *fc106* and *s80* (lane 3). Stage 12 egg chambers showed both forms of *s95* (lane 7) and stage 13 egg chambers displayed both forms of *s60* (lane 13). As predicted, *dec-1* null females carrying two copies of the *fc177TAAG* transgene displayed only the standard forms (lanes 4, 8, and 14). The equivalent intensities of the variant and standard forms in the *w/w; fc177TAAG* egg chambers show that the *fc177TAAG* transgene produces *fc106*, *fc125*, and their derivatives (*s80*, *s60*, and *s95*) at wild type levels.

The failure to detect immunoreactive products with the *Cfc177* antiserum in *dec-1* null mutants carrying the *fc177TAAG* transgene (Fig. 5B, lanes 1 and 2) is consistent with either the absence of *fc177* and its derivatives or the production of a truncated product. To differentiate between these alternatives, it was necessary to identify the amino-terminal fragment produced upon processing of *fc177*. The *fc177* proprotein is processed to *s85* during stages 12 and 13. A *fc177* N-terminal derivative would be expected to appear in a parallel manner. In previous studies, an 85-kDa product was detected in *fs(1)1501* egg chambers with the *Ns80* antiserum (see Fig. 2) whose relative intensity and timing of expression was compatible with a *fc177* N-terminal derivative (Nogueron and Waring, 1995). Since *fc106* is not produced in *fs(1)1501* egg chambers, this 85-kDa product is either a *fc125* or *fc177* derivative. A similar 85-kDa band was detected in stage 12 and 13 egg chambers from wild type and *fs(1)1501* females with the *Cfc106 dec-1* antiserum (Fig. 5C, lanes 5 and 11, and lanes 9 and 10, respectively). A variant form of the 85-kDa band appeared in the appropriate stage specific manner in *w/w* egg chambers (lanes 6 and 12). The 85-kDa species recognized by the *Cfc106* antiserum is distinct from that recognized by the *Nfc177* or *Cfc177* sera as the mobility of *s85*, the 85- kDa C-terminal derivative, was identical in Oregon R and *w/w* egg chambers (data not shown). To determine whether the *fc177TAAG* transgene produced an N-terminal product, stage 12 and 13 egg chambers from *w/w* females carrying two copies of the *fc177TAAG* transgene were analyzed with the *Cfc106* antiserum. As shown in lanes 7 and 13 of Fig. 5C, only the variant form of the 85-kDa N-terminal derivative was evident. The failure to detect either the standard form or an ectopic band in *w/w; fc177TAAG* egg chambers indicates (1) that this 85-kDa product is a *fc177* derivative, and (2) that a stable truncated *fc177* product is not produced by the *fc177* transgene. The detection of a similar 85-kDa band in stage 12 egg chambers from *dec-1* null females carrying two copies of the *fc125TAA* transgene (Fig. 3B, lane 2) provides additional support for its *fc177* origin. Taken together, these data indicate that *dec-1* null females carrying two copies of the *fc177TAAG* transgene (Fig. 5C, lanes 8 and 11) are the equivalent of *fc177* proprotein null mutants.

Ultrastructural analyses showed that *fc177* was critical for the formation of an organized, tripartite endochorion. Autosomal *fc177TAAG* transgenes from two independent transformant lines (3.2.1 and 2.3.1) were introduced into both *fs(1)410* and *fs(1)384 dec-1* null females. As in the null mutants, a continuous layer of electron-dense endochorionic material was evident throughout the main body of stage 14 egg chambers (Fig. 6A and B). Electron-dense accumulations in the interior of the dorsal appendages were also observed (Fig. 6C and D), rather than the reticular-like network characteristic of wild type stage 14 egg chambers. In most sections, the ICL remained associated with the endochorionic material. Neither abnormal association of the ICL with the vitelline membrane nor electron-dense accumulations in the vitelline membrane were observed. These latter observations are consistent with normal production and processing of the *fc106* proprotein in *dec-1* null mutants carrying the *fc177TAAG* transgene.

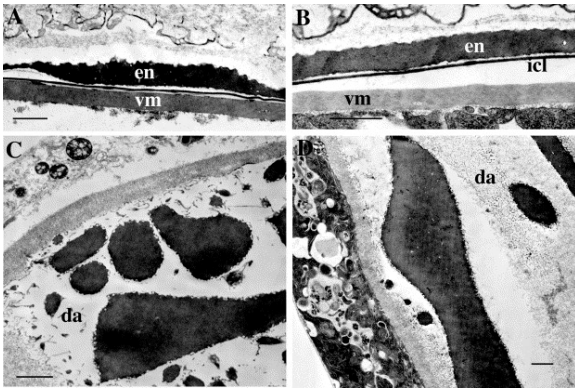


Fig. 6. Fc177 is required for the formation of an organized, tripartite endochorion. Transmission electron micrographs of the eggshell from the main body (A and B) and the interior of a dorsal appendage (C and D) from *dec-1* null mutants carrying two copies of the fc177TAAG [transgene](#). (A and C) fc177TAAG 3.2.1 transgene in *fs(1)384 dec-1* null mutants; (B and D) fc177TAAG 2.3.1 transgene in *fs(1)410 dec-1* null mutant. The bar indicates one micron, and the abbreviations are as previously described.

For functional analyses, transgenes from three independent transformant lines were introduced into *fs(1)410* and *fs(1)384 dec-1* female sterile mutants. The transgene from two lines failed to rescue the female sterile phenotype in both *dec-1* mutant backgrounds. *fs(1)384* females carrying the fc177TAAG transgene from the 3.2.1 transformant line produced a limited number of viable progeny.

Endochorionic material is organized in *dec-1* null mutants that overexpress the fc177 proprotein

To determine whether a tripartite endochorion could be organized in *dec-1* null mutants by the fc177 proprotein alone, a transgene consisting of fc177 cDNA driven by *dec-1* regulatory sequences was introduced into *fs(1)410 dec-1* mutant females. Transmission electron microscopy of stage 14 egg chambers in the main body and dorsal appendage regions revealed near wild-type morphology ([Fig. 7](#)). As expected *fs(1)410; fc177cDNA* females were sterile and produced fragile eggs, indicating that products from other *dec-1* proproteins are required to assemble a functional eggshell. To obtain production of both the fc177 and fc106 proproteins, the fc177cDNA transgene was introduced into *fs(1)410/Df(ct)^{4b1}* heterozygotes. These females were sterile and also produced fragile eggs. This result is consistent with the fc125TAA transgene data and confirms the importance of the fc125-specific sequences in the production of a functional eggshell.

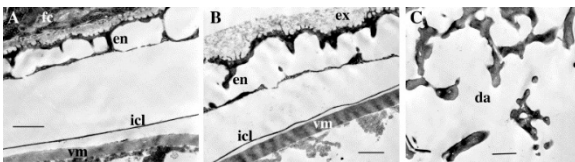


Fig. 7. Near wild-type eggshell morphology in *dec-1* null mutants that overproduce fc177. Transmission electron micrographs of the main body of the eggshell (A and B) from early (A) and later (B) stage 14 egg chamber and the interior of a stage 14 dorsal appendage (C) taken from *fs(1)410* females carrying two copies of the fc177cDNA [transgene](#). The bar indicates one micron and the abbreviations are as previously described.

The *dec-1* gene is transcribed during stages 9–12 with peak accumulation of *dec-1* RNAs occurring during stages 9 and 10. In wild type egg chambers, the alternatively spliced transcript that encodes fc177 is only produced in stage 11 and 12 egg chambers, times when total *dec-1* RNA accumulation has subsided substantially ([Hawley and Waring, 1988](#)). Since the fc177cDNA transgene was driven by *dec-1* regulatory sequences, both premature (stages 9–10) and overexpression of fc177 was expected in *dec-1* null mutants carrying the transgene. To put the

morphological results into a molecular context, it was necessary to determine how the fc177 proprotein was processed in the *dec-1* mutant females. The fc177-specific antiserum Cfc177 (Fig. 8A) was used to monitor processing of the C-terminal sequences. Fig. 8B shows that, as in wild type (lanes 1 and 2), the s85 C-terminal derivative is evident in stage 12/13 egg chambers from *fs(1)410*; fc177cDNA females (lane 3). This demonstrates that C-terminal processing of fc177 is not dependent on either the fc106 or fc125 proproteins. A reactive band of 46 kDa was also observed in both the wild type and mutant egg chambers. Its absence in *fs(1)410* egg chambers (not shown) confirms its *dec-1* identity and suggests that either s85 can be processed to smaller derivatives or that alternative C-terminal processing pathways exist.

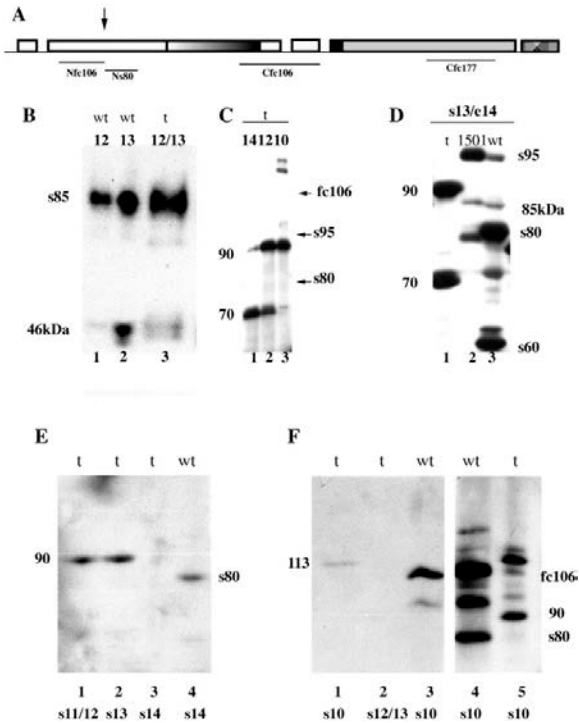


Fig. 8. C- and N-terminal processing of the fc177 proprotein in *dec-1* null mutant egg chambers. (A) Diagram showing *dec-1* open reading frames and the regions used to produce the various *dec-1* antisera. The downward arrow denotes the N terminus of s80, the C-terminal cleavage product of fc106. (B–F) SDS soluble egg chamber proteins from wild type (wt), homozygous *fs(1)410 dec-1* null mutants carrying two copies of the fc177cDNA transgene (t) or *fs(1)1501 dec-1* mutants (1501) were separated by polyacrylamide gel electrophoresis, transferred to nitrocellulose (B–D) or PVDF (E and F), and incubated with the Cfc177 (B), Cfc106 (C, D), Ns80 (E), or Nfc106 antiserum (F, lanes 1–3). In (F), duplicates of lanes 1 and 3 (lanes 5 and 4, respectively) were incubated with the Cfc106 antiserum to mark the positions and insure the presence of the 90-kDa and s80 derivatives. Egg chamber stages are indicated on the top of each lane in (B–D) and at the bottom of each lane in (E) and (F). The C-terminal fc177 derivatives, s85, and a 46-kDa band are indicated in (B); in (C), the positions of fc106, s95, and s80 run in parallel are indicated on the right; the approximate sizes of the N-terminal fc177 derivatives are indicated on the left. (D) High resolution gel showing that the 90- and 70-kDa bands produced by the fc177cDNA transgene (left) do not comigrate with the previously characterized *dec-1* proteins indicated on the right. (E and F) Protein labeling as above; the 113 band indicated in (F) is the approximate size of the largest N-terminal derivative detected in flies carrying the fc177cDNA transgene. Bands in (B), (E), and (F) were detected with ¹²⁵I-Protein A; in (C) and (D), by ECL.

In *fs(1)410*; fc177cDNA egg chambers, the N-terminal derivatives of fc177 can be monitored in the absence of fc106 and fc125 products. Fig. 8C shows fc177 products that are recognized by the Cfc106 antiserum. In stage 10 egg chambers (lane 3), two minor bands in the 113-kDa size range and a prominent product of about 90 kDa

were observed. The 90-kDa band remained prominent and a 70-kDa band emerged during stages 12 and 13 (lane 2). In stage 14 egg chambers, as the 70-kDa band intensified, the 90-kDa band became less intense (lane 1). Hence, while processing of the C-terminal s85 derivative appeared to be normal ([Fig. 8B](#)), processing of the fc177 N-terminal sequences was aberrant. The mobilities of the fc177cDNA derivatives and the 85-kDa fc177 N-terminal derivative are compared in [Fig. 8D](#). Bands that comigrate with the fc177 cDNA derivatives (lane 1) were not observed either in *fs(1)1501* (lane 2) or wild type (lane 3) stage 13 egg chambers. The atypical processing of the fc177 N terminus in *dec-1* null mutants carrying the fc177 cDNA transgene could be due to its premature expression (i.e., stage 10 egg chambers) or the absence of the fc106 and fc125 proproteins. Since similar products are produced by the fc177 cDNA transgene in wild type flies (not shown), the atypical processing is likely to be a consequence of its premature expression. This suggests either that the accessibility of *dec-1* processing sites or the proteolytic machinery involved in processing *dec-1* substrates is different during the early (stage 10) and later (12–13) stages of eggshell assembly.

The stage-specific appearances and the size differences between the immunoreactive fc177cDNA-derived species were reminiscent of fc106 and its derivatives, s80 and s60. The simplest interpretation of these results is that after initial cleavage from the fc177-specific C terminus, the abnormal N terminus is processed like fc106. The 113-kDa band would be equivalent to fc106 with an 8- to 10-kDa C-terminal extension; the 90-kDa band would be similar to s80, and the 70-kDa band would be similar to s60. To extend this parallel, using different antisera, we showed that the immunoreactivities of the predicted fc177 and fc106 counterparts were identical ([Fig. 8](#)). For example, the fc106 proprotein is recognized by all three N-terminal antisera: Nfc106, Ns80, and Cfc106 ([Noguerón and Waring, 1995](#)). Similarly, the 113-kDa fc177 N-terminal derivative reacts with the Nfc106 ([Fig. 8E](#), lane 1), Ns80 (not shown), and Cfc106 ([Fig. 8C](#), lane 3; and [Fig. 8F](#), lane 5) antisera. Like s80 ([Fig. 8E](#), lane 4), the 90-kDa fc177 derivative reacts with the Ns80 antiserum ([Fig. 8E](#), lanes 1 and 2), but not the Nfc106 antiserum ([Fig. 8E](#), lanes 2 and 3). The 70-kDa fc177 band and s60 are both recognized only by the Cfc106 serum. These data suggest that the fc177 cDNA transgene produces fc106-like products in addition to its fc177-specific C-terminal derivative, s85. In wild type egg chambers, fc177 is processed to s85 via a C-terminal 120-kDa intermediate ([Nogueron and Waring, 1995](#)). In the *dec-1* null egg chambers containing the fc177cDNA transgene, the initial cleavage appears to generate s85 and a fc106-like N-terminal fragment rather than the 120-kDa C-terminal processing intermediate and 85-kDa N-terminal fragment. Since endochorion cavities are formed by the fc177 transgene in the absence of a normal fc177 N-terminal derivative, s85 appears to be the critical space-generating component. Furthermore, the production of fc106-like derivatives from the aberrantly cleaved fc177 N terminus is consistent with the near wild type eggshell morphology observed when the fc177cDNA transgene was introduced into *dec-1* null mutants. As shown in [Fig. 1F](#), the production of fc106 is sufficient to prevent the collapse of endochorion material into the underlying vitelline membrane layer.

Discussion

Eggshell proteins are synthesized in a defined temporal order and are secreted into the extracellular space where they organize to form a complex supramolecular structure. The innermost vitelline membrane layer appears morphologically complete by stage 11. The outer chorion layers, ICL and endochorion, begin to form in stage 12, although the tripartite nature of the endochorion is not apparent until late stage 13. A fibrous, biochemically ill-defined outer exochorion is secreted over the chorion layers during stage 14 ([Margaritis, 1985](#)). In *dec-1* egg chambers, morphological aberrations are not apparent until late oogenesis. An organized tripartite endochorion fails to form, and the aggregated endochorionic material that accumulates in the extracellular space eventually collapses into the underlying vitelline membrane. In this study, we have separated aggregation of endochorionic material from its collapse into the underlying vitelline membrane. By removing the fc177-specific C terminus, we created fc177 null *dec-1* mutants with aggregated endochorionic material that was not deposited in the underlying vitelline membrane ([Fig. 6](#)). This indicates that fc177 derivatives are needed for the

production of the floor, pillar, and roof-like architecture of the endochorion, but that the production of fc106, fc125, and their derivatives is sufficient to prevent its collapse. A similar phenotype was observed in the main body of the eggshell in *Df(1)ct^{Ab1}/fs(1)410* trans heterozygotes. The deficiency chromosome produces only fc106 and its derivatives (s25, s20, and s60). The aggregation of endochorionic material in these egg chambers ([Fig. 1A, F](#)) is consistent with the lack of the fc177-specific C-terminal derivatives. The stability of the fused aggregates in the absence of fc125 suggests that production of fc106 and its derivatives is sufficient to prevent the collapse of the endochorion layer. Since s20 is taken up by the oocyte ([Nogueron et al., 2000](#)), it would appear that s25 and/or s60, are the relevant players. Preliminary analysis of transgenes bearing mutations that perturb s25 function suggest that s25 is required to produce a stable endochorion layer ([Mauzy-Melitz, 2001](#)). While unexpected, the near complete morphological rescue of the *dec-1* null phenotype with the fc177cDNA transgene is consistent with this hypothesis. When expressed prematurely in stage 10 egg chambers, an aberrant N-terminal derivative was generated that was processed in a fc106-like manner, yielding s25, s20, and a 70-kDa s60-like derivative. The production of s25 from the fc177 N terminus is compatible with normal ICL morphogenesis and the production of a stable endochorion.

While the ultrastructure of the eggshell in the main body region was similar in the *Df(1)ct^{Ab1}/fs(1)410* and fc177TAAG mutants, electron-dense accumulations were observed in the vitelline membrane near the base of a dorsal appendage in *Df(1)ct^{Ab1}/fs(1)410* stage 14 egg chambers. The localized collapse of the endochorion in *Df(1)ct^{Ab1}/fs(1)410* egg chambers suggests that the elaboration of specialized structures in the anterior pole region may be more sensitive to perturbations in the expression of the *dec-1* derivatives than elaboration of the eggshell in the main body region. The eggshell is produced by a number of different follicle cell subpopulations that differ in their cell migration patterns (reviewed in [Waring, 2000](#)). The main body of the eggshell is elaborated by a large subset of follicle cells that complete their posterior ward migration over the oocyte by late stage 9. During late stage 10, a distinct subset of follicle cells begins to migrate, centripetally, between the nurse cells and the oocyte. These follicle cells are involved in the production of the operculum and micropyle in the anterior region. Two groups of dorsal anterior follicle cells migrate anteriorly during stages 12–14 to form the dorsal appendages. Production of the mRNAs that encode fc106 and fc125 is maximal during stages 9 and 10, and drops precipitously in stage 11 egg chambers. The quantitatively minor fc177 *dec-1* transcript accumulates during stages 11 and 12 ([Hawley and Waring, 1988](#)). Since the production of the dorsal appendages is late, when the accumulation of *dec-1* transcripts is relatively low, N-terminal derivatives may be present in limited quantities in the anterior region. In *Df(1)ct^{Ab1}/fs(1)410* egg chambers, a truncated form of *dec-1* RNA is transcribed from a single allele, and fc106 is the sole source of N-terminal derivatives. The fc177 TAAG egg chambers contained two copies of the fc177TAAG transgene and produced fc106 and its derivatives at wild type levels. A more obvious difference between the fc177TAAG and the *Df(1)ct^{Ab1}/fs(1)410* egg chambers is the production of fc125 in the former. While the selective removal of fc125-specific sequences has no obvious effect on eggshell morphology ([Fig. 4](#)), the stability of the anterior region may be selectively compromised by the simultaneous loss of fc125 and fc177.

Based on morphological data, the tripartite nature of the endochorion in the main body region has been correlated with the secretion of a polysaccharide-rich flocculent material by the overlying follicle cells in late stage 12 egg chambers ([Margaritis, 1986](#)). Cavities filled with flocculent material are created and believed to prevent the fusion of localized deposits of endochorion material. In *dec-1* null mutants, deposits of endochorion material with a pillar-like appearance are observed in early stage 14 egg chambers. In the absence of fc177 derivatives (e.g., s85), the endochorion deposits fuse to form a solid complex. The immunolocalization of s85 within the endochorion cavities ([Nogueron et al., 2000](#)) is consistent with a role in preventing ectopic aggregation. How s85 (and/or the 46-kDa band) prevents aggregation of endochorionic material is not known. It may be an integral part of a scaffold that forms cavities or spaces and prevents endochorion protein complexes in adjacent pillars, and the roof and floor from interacting. In this context, the function of s85 may be akin to

scaffolding proteins that play a critical role in viral assembly (reviewed in [Dokland, 1999](#)). Viral scaffolding proteins provide a transient external brace and internal core around which the viral coat assembles. Viral scaffolding proteins can function in a variety of ways including promoting correct protein–protein interactions, nucleating the assembly of complexes, or preventing formation of improper interactions. While scaffolding proteins have been described primarily in viral systems, they most likely play a general role in macromolecular assembly ([Dokland, 1999](#)). Whereas viral scaffolding proteins are not part of the final structure, if s85 is an eukaryotic counterpart of viral scaffolding proteins, it may persist in the final structure to maintain cavities within the endochorion. The status of s85 has not been examined in the embryo.

An alternative view of how s85 might prevent inappropriate aggregation is that it may bind to an activity in the extracellular space that promotes aggregation of endochorion proteins. Localized binding by s85 in the cavities would restrict aggregation to the pillars, roof and floor. In this context, a collagen fibril aggregation-inhibitor has recently been identified in the sea cucumber dermis ([Trotter et al., 1999](#)). The inhibitor binds to stiparin, a glycoprotein that aggregates collagen fibrils ([Trotter et al., 1996](#)). Irrespective of the molecular mechanism employed, the evolutionarily conserved features of the fc177-specific C terminus are likely to play a prominent role. The fc177-specific C terminus is the most rapidly evolving region of the *dec-1* gene. Alignment of the *D. virilis* and *D. melanogaster dec-1* genes revealed 35% identity in this region ([Badciong et al., 2001](#)). Despite the overall divergence, the fc177-specific C terminus contains two of the most highly conserved features of the *dec-1* proteins: 4 pairs of strictly conserved cysteines (CXC) embedded in a basic subdomain followed by an acidic cluster (pI 4.0), 65 amino acids in length, that shows 94% identity. The functional interchangeability of the *D. virilis* and *D. melanogaster* homologs ([Badciong et al., 2001](#)) underscores the likelihood that these features are instrumental in generating the cavities or spaces that create a tripartite endochorion.

Acknowledgements

We thank Dr. Heather Owens for expert technical assistance and for use of the imaging facility at the University of Wisconsin-Milwaukee and members of Dr. Rosemary Stuart's and our laboratory group for helpful discussions. This work was supported by NIH Grant R15GM55952 (to G.L.W.).

References

- [Aumailley and Gayraud 1998](#) M. Aumailley, B. Gayraud **Structure and biological activity of the extracellular matrix** *J. Mol. Med.*, 76 (1998), pp. 253-265
- [Badciong et al 2001](#) J.C. Badciong, J.M. Otto, G.L. Waring **The functions of the multi-product and rapidly evolving *dec-1* eggshell gene are conserved between evolutionarily distant species of *Drosophila*** *Genetics*, 159 (2001), pp. 1089-1102
- [Bauer and Waring 1987](#) B.J. Bauer, G.L. Waring **7C female sterile mutants fail to accumulate early eggshell proteins necessary for later chorion morphogenesis in *Drosophila*** *Dev. Biol.*, 121 (1987), pp. 349-358
- [Dokland 1999](#) T. Dokland **Scaffolding proteins and their role in viral assembly** *Cell Mol. Life Sci.*, 55 (1999), pp. 580-603
- [Gans et al 1975](#) M. Gans, C. Audit, M. Mason **Isolation and characterization of sex-linked female-sterile mutants in *Drosophila melanogaster*** *Genetics*, 81 (1975), pp. 683-704
- [Hawley and Waring 1988](#) R.J. Hawley, G.L. Waring **Cloning and analysis of the *dec-1* female-sterile locus, a gene required for proper assembly of the *Drosophila* eggshell** *Genes Dev.*, 2 (1988), pp. 341-349
- [Henry and Campbell 1998](#) M.D. Henry, K.P. Campbell **A role for dystroglycan in basement membrane assembly** *Cell*, 95 (1998), pp. 859-870
- [Komitopoulou et al 1988](#) K. Komitopoulou, L.H. Margaritis, F.C. Kafatos **Structural and biochemical studies on four sex-linked chorion mutants of *Drosophila melanogaster*** *Dev. Genet.*, 9 (1988), pp. 37-48

- [Margaritis 1985](#) L.H. Margaritis **Structure and physiology of the eggshell**
G.A. Kerkut, L.I. Gilbert (Eds.), *Comprehensive Insect Physiology, Biochemistry, and Pharmacology*, Vol. 1, Pergamon, Elmsford, NY (1985), pp. 153-230
- [Margaritis 1986](#) L.H. Margaritis **The eggshell of *Drosophila melanogaster*. II. New staging characteristics and fine structural analysis of choriogenesis** *Can. J. Zool.*, 64 (1986), pp. 2152-2175
- [Margaritis et al 1991](#) L.H. Margaritis, S.J. Hamodrakas, I. Papassideri, T. Arad, K.R. Leonard **Three-dimensional reconstruction of innermost chorion layer of *Drosophila grimshawi* and *Drosophila melanogaster* eggshell mutant *fs(1)384*** *Int. J. Biol. Macromol.*, 13 (1991), pp. 247-253
- [Mauzy-Melitz 2001](#) Mauzy-Melitz, D., 2001. Genetic dissection of eggshell assembly in *D. melanogaster*, *in*: Department of Biology. Marquette University, Milwaukee, pp. 226
- [Nogueron et al 2000](#) M.I. Nogueron, D. Mauzy-Melitz, G.L. Waring ***Drosophila dec-1* eggshell proteins are differentially distributed via a multistep extracellular processing and localization pathway** *Dev. Biol.*, 225 (2000), pp. 459-470
- [Noguerón and Waring 1995](#) M.I. Noguerón, G.L. Waring **Regulated processing of *dec-1* eggshell proteins in *Drosophila*** *Dev. Biol.*, 172 (1995), pp. 272-279
- [Savant-Bhonsale and Montell 1993](#) S. Savant-Bhonsale, D.J. Montell **Torso-like encodes the localized determinant of *Drosophila* terminal pattern formation** *Genes Dev.*, 7 (1993), pp. 2548-2555
- [Spradling and Rubin 1982](#) A.C. Spradling, G.M. Rubin **Transposition of cloned P elements into *Drosophila* germ line chromosomes** *Science*, 218 (1982), pp. 341-347
- [St. Johnston and Nusslein-Volhard 1992](#) D. St. Johnston, C. Nusslein-Volhard **The origin of pattern and polarity in the *Drosophila* embryo** *Cell*, 68 (1992), pp. 201-219
- [Trotter et al 1999](#) J.A. Trotter, G. Lyons-Levy, K. Chino, T.J. Koob, D.R. Keene, M.A. Atkinson **Collagen fibril aggregation-inhibitor from sea cucumber dermis** *Matrix Biol.*, 18 (1999), pp. 569-578
- [Trotter et al 1996](#) J.A. Trotter, G. Lyons-Levy, D. Luna, T.J. Koob, D.R. Keene, M.A. Atkinson **Stiparin: a glycoprotein from sea cucumber dermis that aggregates collagen fibrils** *Matrix Biol.*, 15 (1996), pp. 99-110
- [Waring et al 1990](#) G.L. Waring, R.J. Hawley, T. Schoenfeld **Multiple proteins are produced from the *dec-1* eggshell gene in *Drosophila* by alternative RNA splicing and proteolytic cleavage events** *Dev. Biol.*, 142 (1990), pp. 1-12
- [Waring 2000](#) G.L. Waring **Morphogenesis of the eggshell in *Drosophila*** K.W. Jeon (Ed.), *International Review of Cytology*, Academic Press, San Diego (2000), pp. 67-108